Turbulence wave number spectra reconstruction from radial correlation Doppler reflectometry data

E Z Gusakov, M A Irzak, O L Krutkin, A Yu Popov

Ioffe Institute, St Petersburg, Russia

Radial correlation reflectometry (RCR) utilizing simultaneous plasma probing by two microwave beams at slightly different frequencies incident normally upon plasma in the cutoff presence, and correlation analysis of the reflected signals have been used for plasma turbulence characterization in magnetic fusion devices since 90s [1, 2]. This diagnostic benefits from a relative technical simplicity, however the interpretation of the experimental data is complicated by contribution of small-angle-scattering off long-scale fluctuations leading at small turbulence level to substantial overestimation of its correlation length [3].

One of approaches to cope with this problem is so called radial correlation Doppler reflectometry (RCDR), where benefits directly from suppression of the small-angle scattering component in the reflectometer signal, taking place at the oblique enough incidence of the probing wave onto the magnetic surface. This approach was justified in [4] where the expression for the critical incidence angle has been derived. Unfortunately it appears to be dependent on a priori unknown turbulence correlation length, which complicates the RCDR experiment planning and interpretation.

In the present paper based on analytical evaluation of scattering signal the turbulence spectra reconstruction procedure similar to the one developed in [5] and confirmed in [6] for RCR for arbitrary probing angle is proposed. The procedure is validated against the numerical analysis performed utilizing the reciprocity theorem for calculation of the RCDR signal.

In theoretical analysis, linear regime of the probing wave scattering is assumed. Due to strong elongation of the drift-wave turbulence in respect to the magnetic field, O-mode backscattering described by Helmholtz equation is analyzed in 2D geometry:

$$\left\{\Delta+\frac{\omega^2}{c^2}\left(1-\frac{n(q_1)}{n_c}\right)\right\}E_z=\frac{\omega^2}{c^2}\frac{\delta n(q_1,q_2)}{n_c}E_z \qquad (1)$$

Where $n_c=m_e\omega^2/4\pi e^2$ and q_1,q_2 stand for coordinates which are x,y in a slab geometry case and r,φ in case of cylindrical geometry. Based on the reciprocity theorem [7], the amplitude of the backscattering signal in the Born approximation can be represented as follows

$$A_s(\omega) = i\frac{e^2\sqrt{P}}{4m_e\omega}\int_{S_{pol}} \delta n(q_1,q_2)\,E_a^2(q_1,q_2,\omega)\,dq_1dq_2 \tag{2}$$

where P is the probing wave power across the unite length in magnetic field direction, $E_a(q_1,q_2,\omega)$ is the probing wave amplitude at frequency ω corresponding to the unit power launched through the receiving antenna into the unperturbed $(\delta n(q_1,q_2)=0)$ plasma, and S_{pol} stands for the poloidal plasma cross-section. The probing wave electric field E_a here can be represented as a superposition of the partial waves emitted by the antenna and outer boundary conditions for them is given by antenna directivity diagram over poloidal wavenumber. This diagram is assumed to be Gaussian $f(k_{pol},\omega)=(2\sqrt{\pi}\rho)^{1/2}exp[-(k_{pol}-K_\omega)\rho^2/2]$ where k_{pol} is poloidal wavenumber of the partial wave and $K_\omega=\omega sin\vartheta/c$, while ϑ stands for antenna tilting angle with respect to magnetic surface. In case of slab geometry and linear density profile radial structure of partial wave is described by Airy function, whereas in case of cylindrical geometry solution of unperturbed Helmholtz equation in the WKB approximation can be used. Using Fourier representation for the density fluctuation $\delta n(q_1,q_2)$ and performing integration over spatial variables in expression (2), in case of slab geometry and linear density profile, one can derive:

$$A_s(\omega) = \frac{e^2\ell^{3/2}}{m_ec^2}\sqrt{\frac{iP}{\pi}}\int_{-\infty}^{\infty}\frac{d\kappa dq}{2}\delta n_{\kappa,q}\exp(i\Phi)\left[\kappa + i\left(\frac{\kappa L_\omega c}{\omega\rho^2}\frac{2-(qc/\omega)^2}{\sqrt{1-(qc/2\omega)^2}} + \frac{L_\omega c^2}{\omega^2\rho^2}\left(q^2-\kappa^2\right)\right)\right]^{-1/2}$$

$$\Phi = \frac{(\kappa\ell)^3}{12} - L_\omega\kappa + \frac{4}{3}\frac{L_\omega\omega}{c}\left(1-\left(\frac{qc}{2\omega}\right)^2\right)^{3/2} + \kappa q^2\frac{L_\omega c^2}{4\omega^2} + i\frac{(q-2K_\omega)^2\rho^2}{4} \tag{3}$$

Where $l=(L_\omega c^2/\omega^2)^{1/3}$ is the Airy scale, $L_\omega^{-1}=\partial\ln n(x)/\partial x|_{cutoff}$, and κ,q – radial and poloidal wavenumbers of density fluctuation component $\delta n_{\kappa,q}$. In the case of cylinder geometry, amplitude of the scattering signal takes following form:

$$A_s(\omega) = -\frac{e^2\sqrt{P}}{m_e c^2}\frac{1}{\sqrt{\pi}}\int_{-\infty}^{\infty}\int_{-2\omega/c}^{-2\omega/c} dq d\kappa \delta n_{\kappa,q} \frac{\exp(i\Phi\big|_{m=-q/2} - \frac{1}{4}\left(2K+\frac{q}{r_a}\right)^2\rho^2)}{\left(\frac{1}{2}\frac{d^2\Phi}{dm^2}\right)^{1/2}\Big|_{m=-q/2}}\sqrt{\frac{\rho L^3(r_{st})\big|_{m=-q/2}}{\kappa r_a^2}} \quad (4)$$

$$\Phi = \int_{r_c(m)}^{r_a} k_m(r')dr' + \int_{r_c(-q-m)}^{r_a} k_{-q-m}(r')dr' - \frac{\kappa}{|\kappa|}\left(\int_{r_c(-q-m)}^{r_{st}} k_{-q-m}(r')dr' + \int_{r_c(m)}^{r_{st}} k_m(r')dr' + \frac{\pi}{2}\right) + \kappa r_{st}$$

Where $L(r) = \left(\frac{(4m^2-1)}{2r^3} - \frac{\omega^2}{c^2}\frac{d}{dr}\frac{n(r)}{n_c}\right)^{-1/3}$; $k_m(r) = \sqrt{\frac{\omega^2}{c^2}(1-\frac{\overline{n}(r)}{n_c}) - \frac{4m^2-1}{4r^2}}$ is radial component of wave vector of probing wave; r_c - tokamaks minor radius, $r_c(m)$ is the turning point; r_{st} is the point of Bragg resonance, which is defined by relation $k_m(r_{st})+k_{-q-m}(r_{st})=|\kappa|$; In the slab geometry limit, in case of $\kappa << 2\omega/c$ formula (4) coincides with formula (3).

The normalized cross-correlation function of two scattering signals in slightly different frequency channels ω and ω' reads as follows

$$CCF(\Delta\omega) = \frac{< A_S(\omega) A_S^*(\omega') >}{\sqrt{< A_S(\omega) A_S^*(\omega) >< A_S(\omega') A_S^*(\omega') >}} \quad (5)$$

Where $\Delta\omega = \omega' - \omega$, $<...>$ stands for statistical averaging over an ensemble of the fluctuations. Substituting expression (3) or (4) into (5), one can see that the formula for the CCF takes a form of Fourier transform in fluctuation radial wavenumber. Performing the inverse Fourier transformation one can reconstruct the turbulence radial wavenumber spectrum. The formula for such a reconstruction in the case of slab geometry takes a form

$$\left|\delta n_{\kappa,2K_\omega}\right|^2 \propto \left[\kappa^2 + \left(\frac{\kappa L_\omega c}{\omega\rho^2}\frac{2-(2K_\omega c/\omega)^2}{\sqrt{1-(K_\omega c/\omega)^2}} + \frac{L_\omega c^2}{\omega^2\rho^2}\left((2K_\omega)^2 - \kappa^2\right)\right)^2\right]^{1/2} \times \quad (6)$$

$$\times \int_{-\infty}^{\infty} CCF(\Delta x)\exp\left(-i\kappa\Delta x + \frac{1}{2}\left(\frac{\rho\sin\theta}{c}\Delta\omega\right)^2\right)d(\Delta x).$$

Where $\Delta x = 2L_\omega \Delta\omega/\omega$. In the case of cylindrically symmetric plasma expression takes a form

$$\left|\delta n_{\kappa,-2K_\omega r_a}\right|^2 \propto \frac{\left|\kappa r_a^2 \frac{1}{2}\frac{d^2\Phi}{dm^2}(r_{st})\right|_{m=K_\omega r_a}}{L^3(r_{st})} \int_{-\omega/c}^{\omega/c} CCF(\Delta\omega)\times$$
$$\times\exp\left(-2i\kappa'\Delta\omega+\frac{1}{2}\left(\frac{\rho\sin\theta}{c}\Delta\omega\right)^2\right) d\left(\frac{2\omega L(r_{st})^3\Delta\omega}{c^2}\right); \qquad \kappa' = \frac{\kappa}{|\kappa|}\left(\int_{r_c}^{r_{st}(\kappa)} \frac{\omega}{c^2 k_{-q/2}(r')}dr'\right) \tag{7}$$

To validate theoretical analysis, numerical modeling was performed in the case of slab geometry. For a given turbulence CCF $<\delta n(x, y)\delta n(x', y')>= \delta n^2 exp(-(x-x')^2/l_c^2-(y-y')^2/l_c^2)$, CCF was calculated using formula (2), (5) and numerical solution of unperturbed eq. (1). Then reconstruction procedure was used. For the case of $l_c=0.4cm$, $\rho=1.6cm$, $L_\omega=12cm$, and $\vartheta^*=24°$ the scattering signal CCF can be seen on figure 1 while reconstructed CCF can be seen on Figure 2. Significant improvement of agreement after reconstruction can be noted, which validates suggested reconstruction method, but numerical validation in case of cylindrical symmetry is yet to be performed.

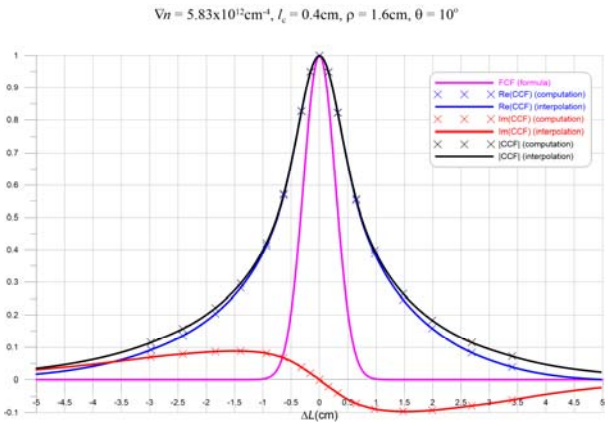

Figure 1: The RCDR *CCF*. Blue - real part, red - imaginary part, black – absolute value, magenta - the turbulence *CCF*. $\vartheta=10°$.

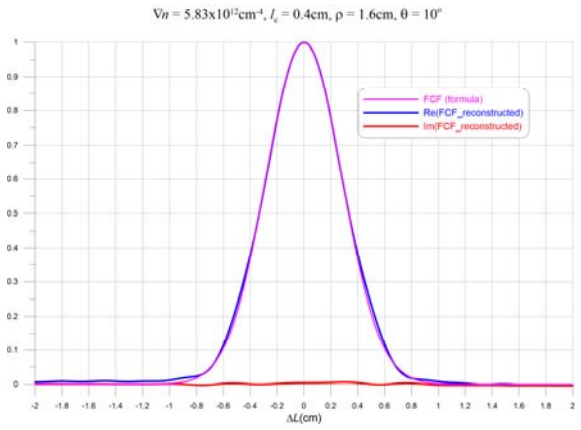

Figure 2: The reconstructed turbulence *CCF*. Blue and red – real and imaginary parts of reconstructed *CCF*; magenta – initial turbulence *CCF*. $\vartheta=10°$.

Financial support of the RSF grant 16-12-10043 is acknowledged.

[1] Costley A, Cripwell P, Prentice R, Sips A C 1990 *Rev Sci. Instrum.* **61** 3487

[2] Mazzucato E, Nazikian R 1993 *Phys.Rev.Lett.* **71** 1840

[3] Gusakov E Z, Tyntarev M A 1997 *Fusion Engineering and Design* **34-35** 501

[4] Gusakov E, Irzak M and Popov A 2014 Plasma Phys. Control. Fusion 56 025009

[5] Gusakov E, Kosolapova N 2011 Plasma Phys. Control. Fusion **53** 045012

[6] Gusakov E, Irzak M, Popov A and Teplova N 2015 Plasma Phys. Control. Fusion

[7] Piliya A D and Popov A Yu 2002 *Plasma Phys. Control. Fusion* **44** 467